

Traveling waves of infection in the Hantavirus epidemics

G. Abramson,^{1,2,*} V. M. Kenkre,^{1,†} T. L. Yates,³ and R. R. Parmenter⁴

¹*Center for Advanced Studies and Department of Physics and Astronomy,
University of New Mexico, Albuquerque, New Mexico 87131*

²*Centro Atómico Bariloche and CONICET, 8400 S. C. de Bariloche, Argentina*

³*Department of Biology and Museum of Southwestern Biology,
University of New Mexico, Albuquerque, New Mexico 87131*

⁴*Sevilleta Long-term Ecological Research Program, Department of Biology,
University of New Mexico, Albuquerque, New Mexico 87131*

(Dated: October 27, 2018)

Traveling waves are analyzed in a model of the Hantavirus infection of deer mice. The existence of two kinds of wave phenomena is predicted. An environmental parameter governs a transition between two regimes of propagation. In one of them the front of infection lags behind at a constant rate. In the other, fronts of susceptible and infected mice travel at the same speed, separated by a constant delay. The dependence of the delay on system parameters is analyzed numerically and through a piecewise linearization.

PACS numbers: 87.19.Xx, 87.23.Cc, 05.45.-a

I. INTRODUCTION

The Hantavirus zoonosis is a persistent problem in many regions of the world [1]. Each species of Hantavirus is almost exclusively associated with a single rodent species from which, eventually, humans may result infected. The disease can range from mild to very severe, with a mortality in excess of 50%. Such is the case of the Hantavirus Pulmonary Syndrome (HPS) produced by the virus associated with the deer mouse (*Peromyscus maniculatus*). In the North American Southwest, indeed, a serious outbreak of this disease in 1993 led to the identification of the virus and its association with the deer mouse [2]. Since then, enormous effort and resources have been devoted to the understanding of the ecology and the epidemiology of the virus-mouse association, with the ultimate goal of being able to predict and prevent the risk for the human population [3, 4].

As observed by Yates et al. [5], the role of the environment seems to be determinant in the prevalence of the infection within the mouse population, and the related incidence of the HPS. Its has been observed that the disease can disappear completely from a local population during times of adverse environmental conditions, only to reappear sporadically [3, 6]. Besides, there are indications of focality of the infection in “refugia” of the mouse population. Both phenomena are most probably related, the refugia acting as reservoirs of the virus during times when the infection has disappeared from most of the landscape. When environmental conditions change, the infection spreads again from these refugia.

In a recent work [7], Abramson and Kenkre have shown that a simple epidemic model is able to display qualita-

tively these behaviors, as the result of a bifurcation of the equilibrium states of the system as controlled by the carrying capacity of the medium. The purpose of the present paper is to analyze the dynamics of simple traveling waves, as a model of the mechanisms in which an epidemic wave of Hantavirus might propagate into a previously uninfected region.

II. SPATIALLY EXTENDED MODEL

The model of Ref. [7] is a mean-field continuous model which has been intentionally kept simple enough to facilitate the comprehension of the basic mechanisms, and at the same time to incorporate as many known facts about the ecology and epidemiology of the biological system as possible. The reader is referred to [7] for a detailed discussion, which we summarize here. It is known that the virus does not affect properties such as the mortality of the mice, so that no appreciable difference in death rate, for example, is to be expected between susceptible and infected mice. It is also not transmitted to newborns, so that all mice are born susceptible. The infection is transmitted from mouse to mouse through individual contacts, presumably during fights. More general facts of the ecology of *Peromyscus* indicate that adults occasionally shift their home range to nearby locations, in particular if these are vacant [8, 9]. This enables us to model the transport of mice as a diffusion process. Finally, intra-species competition for resources indicate a saturated population growth, which has been observed to be of a logistic form in the laboratory [10]. Logistic growth is also a well established metaphor of the dynamics of a self-limitating population [11].

For the sake of simplicity, assume further that the only population structure is the division of the whole population into susceptible and infected mice, denoted by M_S and M_I respectively. With these ingredients, the model

*Electronic address: abramson@cab.cnea.gov.ar

†Electronic address: kenkre@unm.edu

is described by the following equations:

$$\frac{\partial M_S}{\partial t} = bM - cM_S - \frac{M_S M}{K(x, t)} - aM_S M_I + D\nabla^2 M_S \quad (1)$$

$$\frac{\partial M_I}{\partial t} = -cM_I - \frac{M_I M}{K(x, t)} + aM_S M_I + D\nabla^2 M_S. \quad (2)$$

Observe that the carrying capacity $K(x, t)$, containing the most direct effect of the environment on the mouse population, is allowed, in our model, a spatial and a temporal variation, to accommodate for a diversity of habitats and temporal phenomena. The latter comprise the yearly variation due to seasonality, but also sporadic fluctuations such as droughts and El Niño effects.

The sum of the two equations (1)-(2) reduces to a single equation for the whole population:

$$\frac{\partial M}{\partial t} = (b - c)M \left(1 - \frac{M}{(b - c)K} \right) + D\nabla^2 M. \quad (3)$$

This is Fisher's equation, originally proposed as a deterministic model of the spread of a favored gene in a population [12], and which eventually became a standard model for a self regulated field in a diversity of situations [11, 13].

In Ref. [7] it was shown that, as a function of K , the system undergoes a bifurcation between a stable state with only susceptible mice (and $M_I = 0$) to a stable state with both positive populations. The value of the critical carrying capacity is a function of the parameters in the following way:

$$K_c = \frac{b}{a(b - c)}. \quad (4)$$

This critical value does not depend on D , and the same bifurcation is observed either in a space-independent system ($D = 0$) or in a homogeneous extended one in the presence of diffusion. In an inhomogeneous situation, for moderate values of the diffusion coefficient, the infected subpopulation remains restricted to those places where $K > K_c$, becoming extinct in the rest. During times of adverse environmental conditions, these regions become isolated and constitute the observed refugia. Figure 1 shows a typical situation of this phenomenon. A simulated, albeit realistic, landscape of $K(x)$ has been derived from satellite images in Northern Patagonia. The carrying capacity is supposed proportional to the vegetation cover, and results highest along a river, clearly inferred from the density plots. These show the distribution of the populations of susceptible and infected mice. It can be seen that susceptible mice cover most of the range. Meanwhile, the infected population has become extinct in most of it, and persists only in some of the places of highest K . The distributions shown in Fig. 1 constitute a stable equilibrium of the system, found by numerical resolution of Eqs. (1)-(2) from an arbitrary initial condition, and with zero-current boundary conditions.

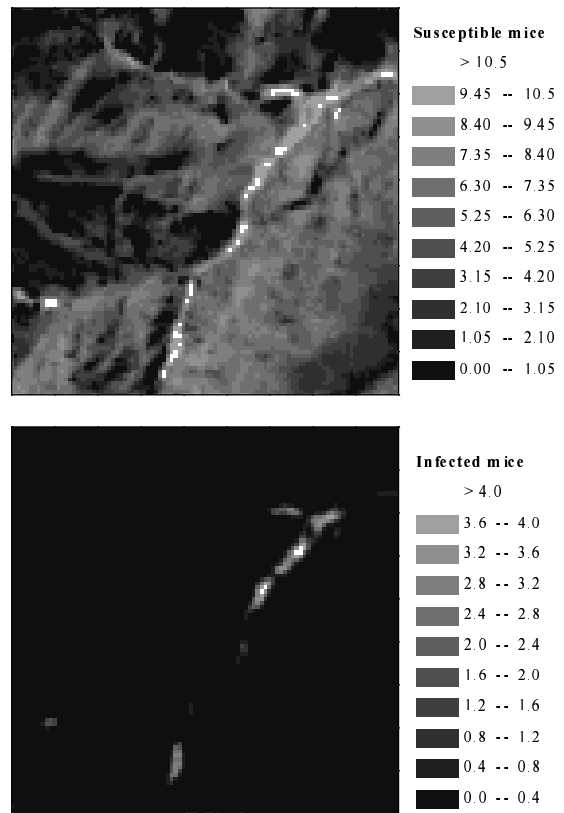


FIG. 1: Density plots showing characteristic distribution of susceptible and infected mice in an inhomogeneous landscape, where the carrying capacity has been modeled according to the vegetation, derived from satellite imagery.

III. TRAVELING WAVES

When conditions in the landscape change, how do the infected phase evolve from the refugia, retracting from or, more importantly, invading previously uninfected regions? this is the primary question we address in the present paper. Fisher's equation (3) has found wide applicability for the description of the formation and propagation of spatio-temporal patterns. Traveling wave solutions of Fisher's equation paradigmatically show how a stable phase invades an unstable one in the form of a front propagating at a certain speed.

There is no reason to suppose *a priori* that the two waves, susceptible and infective, will travel at the same speed. Accordingly, we use an ansatz which incorporates two independent traveling waves. In one dimension, $z_1 = x - v_S t$ in Eq. (1) and $z_2 = x - v_I t$ in Eq. (2). This gives the following second-order system of ordinary differential equations:

$$D \frac{d^2 M_S(z_1)}{dz_1^2} + v_S \frac{dM_S(z_1)}{dz_1} + f(M_S, M_I) = 0, \quad (5)$$

$$D \frac{d^2 M_I(z_2)}{dz_2^2} + v_I \frac{dM_I(z_2)}{dz_2} + g(M_S, M_I) = 0, \quad (6)$$

where v_S and v_I are the speeds of the susceptible and infected waves respectively, and f and g are the non-diffusive term in (1)-(2).

There are two interesting scenarios for these waves. In the first one, a large part of the system is initially at a state of low carrying capacity, below K_c , and consequently the population consists of uninfected mice only, at the stable equilibrium. Let us suppose that this region is in contact with a refugium. If environmental changes occur, and the whole region finds itself at a value of the carrying capacity $K > K_c$, the population will be out of equilibrium. Two processes will occur simultaneously: the population of susceptible mice will evolve towards a new equilibrium, and a wave of infected mice will advance from the refugium, invading the susceptible population. The speed of this wave can be calculated from the stability analysis of the equilibrium states, requiring that the unstable infected mice density does not oscillate below zero. This unstable equilibrium is $M_S^* = K(b - c)$, $M_I^* = 0$, and a linear stability analysis of the system (5)-(6) provides the following four eigenvalues:

$$\lambda_{1,2} = \frac{-v \pm \sqrt{v^2 + 4D(b - c)}}{2D}, \quad (7)$$

$$\lambda_{3,4} = \frac{-v \pm \sqrt{v^2 + 4D[b - aK(b - c)]}}{2D}. \quad (8)$$

The requirement that $M_I(z)$ does not oscillate below 0 imposes a restriction to the radical in Eq. (8), from which we find the following expression for the speed of the traveling wave:

$$v \geq 2\sqrt{D[-b + aK(b - c)]}. \quad (9)$$

An example of such a wave is shown in Fig. 2a, found by a numerical integration of Eqs. (1) and (2) in 1 dimension.

The second interesting scenario corresponds to a system which is initially empty of mice, both susceptible and infected. This situation is always unstable within the validity of our simple model, but it is certainly a biological possibility. Consider a system with $K > K_c$, and with $M_S = M_I = 0$ in almost all of its range, but in contact with a refugium in equilibrium. A wave of both mice populations will develop invading the empty region. In fact, the total population will display just the behavior of a traveling wave of Fisher's equation. This wave will be composed of two fronts, susceptible and infected respectively, with a delay of the latter with respect to the former. As before, we can find the speeds of these two waves from a stability analysis around the corresponding equilibria. The leading wave propagates into the null equilibrium, $M_S^* = M_I^* = 0$, to which the following eigenvalues correspond:

$$\mu_{1,2} = \frac{-v_I \pm \sqrt{v_I^2 + 4Dc}}{2D}, \quad (10)$$

$$\mu_{3,4} = \frac{-v_S \pm \sqrt{v_S^2 - 4D(b - c)}}{2D}. \quad (11)$$

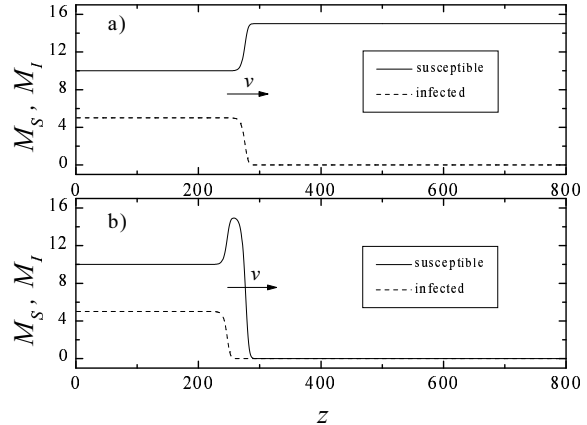


FIG. 2: Traveling waves in the one dimensional model. a) Infection wave invading a noninfected population. b) Noninfected mice invading an empty region, followed by an infection wave. Model parameters: $a = 0.1$, $b = 1$, $c = 0.5$, $D = 1$, $K = 30$. Both waves move at the same speed $v = \sqrt{2}$ for this choice of parameters.

In this situations, we require that $M_S(z)$ does not oscillate below 0, and Eq. (11) provides the restriction on the speed of the susceptible front:

$$v_S \geq 2\sqrt{D(b - c)}, \quad (12)$$

which is, naturally, the same result as for Fisher's equation. The second front, developed when part of the quasi-stable population of susceptible mice is converted into infected, evolves from the equilibrium $M_S^* = K(b - c)$, $M_I^* = 0$, as in the previous scenario. Consequently, the same linear stability analysis apply, and from Eq. (8) we find a speed analogous to Eq. (9). The front of infected move behind the susceptible one at a speed:

$$v_I \geq 2\sqrt{D[-b + aK(b - c)]}, \quad (13)$$

which, unlike v_S , does depend on the contagion rate a and the carrying capacity K . Figure 2b shows such a situation. The density of susceptible mice rises from zero and lingers near the positive unstable equilibrium before tending to the stable one. It is remarkable that a delay exists between the two fronts, even when no such effect was explicitly considered in the dynamics (such as incubation time, or age dependence). Such delays have been observed in some populations and rationalized in different ways (see [14] or [3] for a synthesis).

Even though Eqs. (9), (12) and (13) give only a lower bound to the speed of propagation of the fronts, and allow a continuous of speeds above this, in real situations only the lower bound is expected to be observed as a stationary solution. Higher speeds may, however, play a role in transient situations whose relevance in far from equilibrium systems such as real mice in the wild, subject to a fluctuating environment, cannot be underestimated.

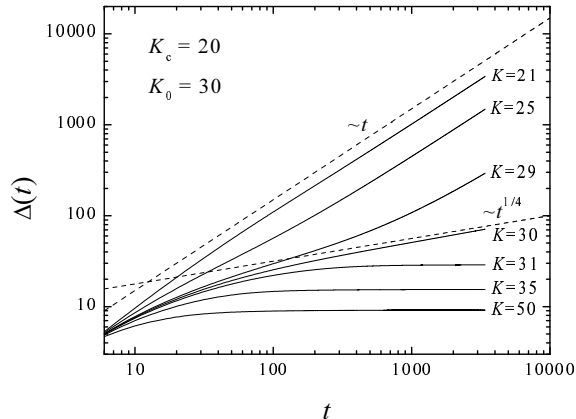


FIG. 3: Delay of the infected front, as a function of time, following an initial condition as described in the text. Two regimes are shown: $K_c < K < K_0$ and $K_0 < K$, separated by the critical case $K = K_0$, that behaves asymptotically as $t^{1/4}$.

The different functional dependence of v_S and v_I on the parameters of the system (Eqs. (12)-(13)) indicates that two regimes are possible. Indeed, when $v_I < v_S$ the front of infection lags behind the front of susceptible at a delay Δ that increases linearly in time: $\Delta(t) = (v_S - v_I)t$. Elementary manipulation of Eqs. (12) and (13) shows that this occurs whenever the carrying capacity satisfies:

$$K_c < K < K_0 \equiv \frac{2b - c}{a(b - c)} \quad (14)$$

where K_0 is a new critical carrying capacity. At $K = K_0$ the delay becomes effectively constant. For values of K greater than K_0 , the velocities v_I and v_S , calculated from linear considerations around the equilibria, satisfy $v_I > v_S$. This regime is clearly unphysical in a stationary situation, since the front of susceptible necessarily precedes the infected one. It could be realizable and relevant in transient situations, that will be analyzed elsewhere. From numerical resolution of the system, we can observe that $v_I \rightarrow v_S$ and the delay tends to a constant value, whenever $K > K_0$. Figure 3 shows the temporal evolution of the delay in the two regimes $K < K_0$ and $K > K_0$, as well as in the critical case $K = K_0$, where it is seen to increase as $\Delta \sim t^{1/4}$. It can be seen that there is a transient time in both regimes, that gets progressively longer as K approaches K_0 either from above or from below.

With the assumption that $v_S = v_I = v$, it is possible to perform a piecewise linearization of Eqs. (5)-(6) and find an approximate analytical expression for the front shapes shown in Fig. 2b and, consequently, for the delay Δ in the stationary state. The details of the calculation can be found in the Appendix. The main result is the following expression for the delay, for the case of equal

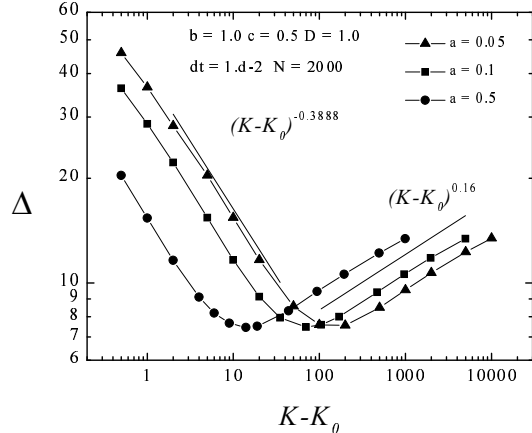


FIG. 4: Delay of the infected front, as a function of K .

speeds of the two classes of mice:

$$\Delta = \frac{\sqrt{D}}{i\sqrt{(b-c)a(K-K_0)}} \log(w_1 w_2), \quad (15)$$

where w_1 and w_2 are complex numbers of unit modulus that depend on a , b and c , so that the logarithm is effectively twice the phase difference between them. When $K \rightarrow K_0^+$, the arguments of w_1 and w_2 tend to π and 0 respectively, so that the following critical behavior is predicted by the linear approximation:

$$\Delta \sim \sqrt{D}[(b-c)a(K-K_0)]^{-1/2}, \quad \text{when } K \rightarrow K_0^+. \quad (16)$$

We have analyzed the dependence of Δ on K by means of numerical resolution of the full system. In Fig. 4 we plot the asymptotic value of Δ as a function of $K - K_0$ for a variety of system parameters. The behavior is found to be

$$\Delta \sim \sqrt{D}[(b-c)a(K-K_0)]^{-\alpha} \quad (17)$$

for values of K immediately above K_0 . The exponent α is parameter-independent, and its value, calculated from the simulations is, approximately 0.388. There is a discrepancy in the exponent found numerically in the fully nonlinear system and the one found in the linearized approximation, which shows the limitation of the linearized solution.

This critical behavior of the delay persists while the wavefronts are of the kind shown in Fig. 2b. However, if K continues to grow the equilibrium value of the infected population turns greater than the equilibrium value of the susceptible. There is a gradual crossover to a situation where most of the population becomes infected. The value of the carrying capacity at which this happens can be estimated from the known equilibria, $M_S^* = M_I^*$, giving:

$$K_1 = \frac{2b}{a(b-c)}. \quad (18)$$

Indeed, the numerical results show that the power law decay of the delay as a function of K starts to flatten for values of $K > K_1$ and reaches a minimum which shows the same a^{-1} dependence that K_1 does. Greater values of K are probably unrealistic in the arid and semi-arid habitats of the Southwest. It is nevertheless interesting to point out that the interaction of the two fronts in this regime results in an *increase* of the delay as a function of K . This increase is also algebraic:

$$\Delta \sim (K - K_0)^\beta, \quad (19)$$

with $\beta \approx 0.16$, as found in the numerical calculations.

IV. CONCLUSION

We have analyzed the propagation of traveling fronts in 1 dimension in a simple model of the ecology and epidemiology of the Hantavirus in deer mouse. We have found that, when a mouse-free region is in contact with an infected region in equilibrium, two waves propagate into the empty region. The first one is a wave of susceptible mice. A wave of infected mice propagates behind it with a certain delay. Two regimes of propagation exist, controlled by the environmental parameter K . If $K_c < K < K_0$, the lag between the two fronts increase linearly in time. Conversely, if $K > K_0$, the two fronts propagate at the same speed and the delay depends critically on the difference $K - K_0$.

The occurrence of this double regime may be of relevance for the control of the propagation of an epidemic wave. Indeed, the controlled reduction of K ahead of a propagating wave seems the most effective mean of stopping or reducing its advance. Ideally, the carrying capacity should be reduced below K_0 , to ensure the complete extinction of the infection. However, if such a reduction is not feasible, the fact that $K_0 > K_c$ provides an alternative: a reduction of the carrying capacity below K_0 would make the wave of infection start to lag more and more behind the wave of healthy mice. Possible implementations of these strategies, based on the propagation of waves in the presence of ‘‘barriers,’’ will be analyzed in detail elsewhere.

The existence of dynamical phenomena such as these traveling fronts also opens the interesting possibility of subjecting our predictions to experimental verification. Controlled experiments of front propagation could be possible in the Sevilleta LTER facility, that the University of New Mexico operates near Socorro, NM [15]. Measurements of uncontrolled mice populations along lines radiating from the refugia of infection will also provide evidence of the propagation mechanisms. The observation of these in real mice population will provide a valuable source of data to assign realistic values to the parameters of the mathematical model.

Acknowledgments

V. M. K. and G. A. acknowledge many discussions with Fred Koster and Jorge Salazar from which we learnt much regarding the peculiarities of the Hantavirus. We also thank Greg Glass, Karl Johnson, Luca Giuggioli and María Alejandra Aguirre for discussions. V. M. K. acknowledges a contract from the Los Alamos National Laboratory to the University of New Mexico and a grant from the National Science Foundation’s Division of Materials Research (DMR0097204). G. A. thanks the support of the Consortium of the Americas for Interdisciplinary Science and the hospitality of the University of New Mexico. A part of the numerically intensive computations was carried out on the Albuquerque High Performance Computing Center facilities.

V. APPENDIX: LINEARIZED SOLUTIONS

For the purpose of finding approximate solutions of the waves profiles, it is better to replace the system (5)-(6) with one involving M and M_I instead:

$$DM'' + vM' + (b - c)M - \frac{M^2}{K} = 0, \quad (20)$$

$$DM_I'' + vM_I' + q(M)M_I - aM_I^2 = 0, \quad (21)$$

where $q(M(z)) = -c + aM(z) - M(z)/K$ and both speeds are assumed equal, as observed in numerical resolutions for the regime $K > K_0$. Primes denote differentiation with respect to z . The reason for using this system is that the equation for $M(z)$, Eq. (20), being closed, can be solved independently of M_I . Its solution can be used then into Eq. (21) as a z -dependent parameter and solve for $M_I(z)$.

Linearized solutions for the traveling waves of Fisher’s equation (20) are well known, and essentially consist of two exponentials, matched smoothly at $z = 0$, representing a front that travels to the right at a speed $v \geq 2\sqrt{D(b - c)}$. Such a function needs a further simplification in order to solve Eq. (21). We approximate $M(z)$ with a step function discontinuous at $z = 0$: $M(z) = M^* = K(b - c)$ if $z < 0$ and $M(z) = 0$ if $z > 0$. Consequently, we have that $q(z) = aM_I^* = -b + aK(b - c)$ if $z < 0$ and $q(z) = -c$ if $z > 0$. We also linearize on both sides of the center value $M_I(-\Delta) = M_I^*/2$, which defines Δ as the delay between the two waves. Figure 5 shows the geometry of the procedure. The linearized equation for M_I breaks into three regimes:

$$DM_I'' + vM_I' - a(M_I - M_I^*) = 0 \text{ if } z < -\Delta, \quad (22)$$

$$DM_I'' + vM_I' + aM_I^*M_I = 0 \text{ if } z \in [-\Delta, 0], \quad (23)$$

$$DM_I'' + vM_I' - CM_I = 0 \text{ if } 0 < z. \quad (24)$$

The solutions of these are respectively:

$$M_1(z) = -\frac{b}{a} + K(b - c) + a_1 e^{\lambda z} \text{ if } z < -\Delta, \quad (25)$$

$$M_2(z) = b_1 e^{\mu_+ z} + b_2 e^{\mu_- z} \quad \text{if } z \in [-\Delta, 0], (26)$$

$$M_3(z) = c_1 e^{\nu z} \quad \text{if } 0 < z, \quad (27)$$

where:

$$\lambda = \frac{\sqrt{b-c+a} - \sqrt{b-c}}{\sqrt{D}}, \quad (28)$$

$$\mu_{\pm} = -\sqrt{\frac{b-c}{D}} \pm i\sqrt{\frac{b-c}{D}a(K-K_0)}, \quad (29)$$

$$\nu = -\frac{\sqrt{b-c} + \sqrt{b}}{\sqrt{D}}, \quad (30)$$

and the terms that diverge in infinity have already been cancelled. It is clear that $\lambda > 0$ and $\nu < 0$, as required for the solution not to diverge in $\mp\infty$. The real part of μ_{\pm} is always positive, and there is an imaginary part when $K > K_0$.

The solutions M_1 , M_2 and M_3 need to be matched smoothly at $z = -\Delta$ and $z = 0$, in the following way ($r = b - c$ from now on):

$$M_1(-\Delta) = -\frac{b}{2a} + \frac{kr}{2}, \quad (31)$$

$$M_2(-\Delta) = -\frac{b}{2a} + \frac{kr}{2}, \quad (32)$$

$$M_1'(-\Delta) = M_2'(-\Delta), \quad (33)$$

$$M_2(0) = M_3(0), \quad (34)$$

$$M_2'(0) = M_3'(0). \quad (35)$$

These are five equations with five unknowns that can be solved without difficulty:

$$a_1 = -\frac{-b/a + kr}{2} e^{\lambda\Delta}, \quad (36)$$

$$b_1 = -\frac{(\lambda + \mu_-)}{2(\mu_+ - \mu_-)} (kr - b/a) e^{\mu_+\Delta}, \quad (37)$$

$$b_2 = -\frac{(\lambda + \mu_+)}{2(\mu_+ - \mu_-)} (kr - b/a) e^{\mu_-\Delta}, \quad (38)$$

$$c_1 = b_1 + b_2, \quad (39)$$

and:

$$\Delta = \frac{1}{\mu_+ - \mu_-} \log \left[\frac{(\lambda + \mu_+)(\mu_- - \nu)}{(\lambda + \mu_-)(\mu_+ - \nu)} \right]. \quad (40)$$

Expressions (25)-(27), (28)-(30) and (36)-(40) define the linearized solution for M_I . An example of such a front wave is shown in Fig. 5.

Using expressions (28)-(30) in (40), it easy to see find:

$$\Delta = \frac{\sqrt{D}}{i\sqrt{(b-c)a(K-K_0)}} \log(w_1 w_2), \quad (41)$$

where

$$w_1 = \frac{\lambda + \mu_+}{\lambda + \mu_-} \equiv e^{i\phi_1}, \quad (42)$$

$$w_2 = \frac{\mu_- - \nu}{\mu_+ - \nu} \equiv e^{-i\phi_2}, \quad (43)$$

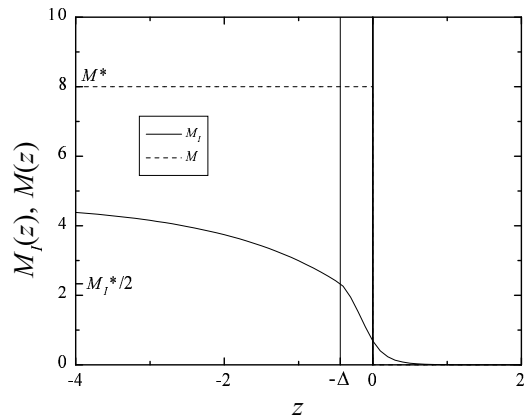


FIG. 5: Linearized solutions. System parameters are: $a = 0.3$, $b = 1$, $c = 0.5$, $K = 16$, $D = 0.1$.

where ϕ_1 and ϕ_2 are respectively the arguments of the complex numbers $\lambda + \mu_+$ and $\mu_+ - \nu$. It is easy to see that ϕ_1 and ϕ_2 do not depend on D , so that the logarithm only corrects the dependence of Δ on $(b-c)a(K-K_0)$. It can be also easily observed that w_1 lies in the second quadrant, and w_2 in the fourth, and that $\text{Im } w_1 = -\text{Im } w_2$. When $K \rightarrow K_0^+$, the imaginary parts tend to zero and the phase difference between both tend to π . Consequently the leading behavior of Δ results:

$$\Delta \sim \sqrt{D} [(b-c)a(K-K_0)]^{-1/2}. \quad (44)$$

This result from the piecewise linearization does not agree with that found numerically in the nonlinear system.

-
- [1] J. N. Mills, T. L. Yates, T. G. Ksiazek, C. J. Peters and J. E. Childs, *Emerging Infectious Diseases* **5**, 95 (1999).
 [2] Sevilleta LTER Publication No. 41 (1993).
 [3] J. N. Mills, T. G. Ksiazek, C. J. Peters and J. E. Childs, *Emerging Infectious Diseases* **5**, 135 (1999).

- [4] C. A. Parmenter, T. Yates, R. R. Parmenter, J. N. Mills, J. E. Childs, M. L. Campbell, J. L. Dunnum and J. Milner, *J. of Wildlife diseases* **34**, 1 (1998).
 [5] T. Yates *et al.*, *Bioscience*, to be published (2002).
 [6] C. A. Parmenter, T. L. Yates, R. R. Parmenter and J. L.

- Dunnum, *Emerging Infectious Diseases* **5**, 118 (1999).
- [7] G. Abramson and V. M. Kenkre, arXiv.org e-Print archive, preprint arXiv:physics/0202035 (2002).
- [8] L. F. Stickel, in *Biology of Peromyscus (Rodentia)*, J. A. King (editor) (The American Society of Mammalogists, Special publication No. 2, 1968)
- [9] S. H. Vessey, *American Zoologist* **27**, 879 (1987).
- [10] C. R. Terman, in *Biology of Peromyscus (Rodentia)*, J. A. King (editor) (The American Society of Mammalogists, Special publication No. 2, 1968)
- [11] J. D. Murray, *Mathematical Biology*, 2nd ed. (Springer, New York, 1993).
- [12] R. A. Fisher, *Ann. Eugen.* **7**, 355 (1936).
- [13] G. Abramson, A. R. Bishop, and V. M. Kenkre, *Physical Review E* **64**, 066615 (2001).
- [14] S. K. Morgan Ernest, J. H. Brown and R. R. Parmenter, *Oikos* **88**, 470 (2000).
- [15] Sevilleta Long-Term Ecological Research Program (LTER), <http://sevilleta.unm.edu>.